Bioorganic & Medicinal Chemistry Letters xxx (2016) xxx-xxx

Contents lists available at ScienceDirect

Bioorganic & Medicinal Chemistry Letters

journal homepage: www.elsevier.com

Cyclic ferrocenylnaphthalene diimide derivative as a new class of G-quadruplex DNA binding ligand

Md. Monirul Islam [a], Shinobu Sato [a, b], Shingo Shinozaki [a], Shigeori Takenaka [a, b, *]

[a] Department of Applied Chemistry, Kyushu Institute of Technology, Kitakyushu 804-8550, Japan
[b] Center for Bio-microsensing Technology, Kyushu Institute of Technology, Kitakyushu 804-8550, Japan

ARTICLE INFO

Article history:
Received 6 August 2016
Received in revised form 19 October 2016
Accepted 11 November 2016
Available online xxx

Keywords:
Cyclic ferrocenylnaphthalene diimide
Tetraplex DNA binder
G-quadruplexes DNA
Human telomere DNA
Promotor region
Thrombin binding aptamer
Double stranded DNA

ABSTRACT

To identify an effective ligand that binds to a G-quadruplex structure but not a double-stranded DNA (dsDNA), a set of biophysical and biochemical experiments were carried out using newly synthesized cyclic ferrocenylnaphthalene diimide (cFNDI, **1**) or the non-cyclic derivative (**2**) with various structures of G-quadruplex DNAs and dsDNA. Compound **1** bound strongly to G-quadruplexes DNAs (10^6 M^{-1} order) with diminished binding to dsDNA (10^4 M^{-1} order) in 100 mM AcOH-AcOK buffer (pH 5.5) containing 100 mM KCl. Interestingly, **1** showed an approximately 50-fold higher selectivity to mixed hybrid-type telomeric G-quadruplex DNA ($K = 3.4 \times 10^6$ M^{-1} and a 2:1 stoichiometry) than dsDNA ($K = 7.5 \times 10^4$ M^{-1}) did. Furthermore, **1** showed higher thermal stability to G-quadruplex DNAs than it did to dsDNA with a preference for *c-kit* and *c-myc* G-quadruplex DNAs over telomeric and thrombin binding aptamers. Additionally, **1** exhibited telomerase inhibitory activity with a half-maximal inhibitory concentration (IC_{50}) of 0.4 μM. Compound **2** showed a preference for G-quadruplex; however, the binding affinity magnitude and preference were improved in **1** because the former had a cyclic structure.

G-quadruplex-forming sequences occur at the ends of eukaryotic chromosomes and are known as telomeres, and they also exist in other vital regions of the genome as oncogene promoters, introns, 5′-UTR regions, or aptamers.[1–3] The G-quadruplex is a four-stranded nucleic acid structure produced by guanine-rich repeating sequences such as TTAGGG, which are composed of π-π-stacked on guanine tetrads (G-tetrads) by Hoogsteen-bonds.[2] The structure, stability, and topology of G-quadruplex DNAs depend on numerous factors such as the sequence, length of the loops, and mainly the presenting metal ions.[3] For instance, the human telomeric DNA can fold into a mixture of G-quadruplex topologies (parallel, antiparallel, and hybrid) in vitro under physiological conditions, compared to duplex DNAs.[4] The formation of G-quadruplex structures can regulate the transcriptional and translational activity of telomerase, expression of oncogenes, or both in the body. The telomere contains the length of the telomere DNA and is involved in approximately 85% of all cancers.

Molecules that stabilize G-quadruplex structures can inhibit telomerase or oncogene activities, or both and, thereby, inhibit intermittent cancer progression.[5] These molecules are considered potential anticancer therapeutic agents.[6–9] Notably, G-quadruplex-forming activity is very low in human somatic cells. Therefore, one of the major challenges in this field is to design a suitable new molecule as a ligand that selectively binds to G-quadruplex over dsDNA and exhibits ligand specificity toward a particular G-quadruplex topology.

Numerous ligands that preferentially bind G-quadruplex DNAs over duplex DNA have been reported over the past few decades. These ligands are well studied as G-quadruplex stabilizers both in vitro and in vivo that exhibit anticancer activity.[6–8] However, their binding affinities are still nonselective, as they show affinity to duplexes and other structures. Previously, we reported the synthesis and interaction studies of numerous cyclic naphthalene diimide (NDI) derivatives with G-quadruplex DNAs and dsDNA.[10–13] Furthermore, other macrocyclic NDI derivatives have been synthesized and studied by Marchetti et al.[14] to investigate their interaction with DNAs. These cyclic ligands showed versatile binding characteristics to G-quadruplex DNAs and dsDNA. We had numerous questions about the selectivity of these ligands to G-quadruplex DNAs over dsDNA including cyclic ligands with substituents or chain variations. These cyclic ligands were synthesized by cyclization with benzene or cyclohexane ring with two types of connecting chains (Fig. 1).

We hypothesized that these rings might have some beneficial or harmful effects on their binding with G-quadruplex DNAs or dsDNA, respectively. Particularly, the cyclohexane fused ring structure is more flexible during the binding with dsDNA than it is with other DNAs. It cannot contribute to the intercalation with dsDNA, but it may be partially stacked on dsDNA, which consequently reduces binding with dsDNA. However, the cyclohexane rings in cyclic ligands do not have beneficial effects on their binding with G-quadruplex DNAs because the interaction between the cyclohexane ring and the loop part of the G-quadruplex DNAs has no positive effect. On the other hand, the benzene ring in cyclic ligands may have a suitable effect on their binding with G-quadruplex DNAs be-

* Corresponding author at: Department of Applied Chemistry, Kyushu Institute of Technology, Kitakyushu 804-8550, Japan.
Email address: shige@che.kyutech.ac.jp (S. Takenaka)

http://dx.doi.org/10.1016/j.bmcl.2016.11.037
0960-894/

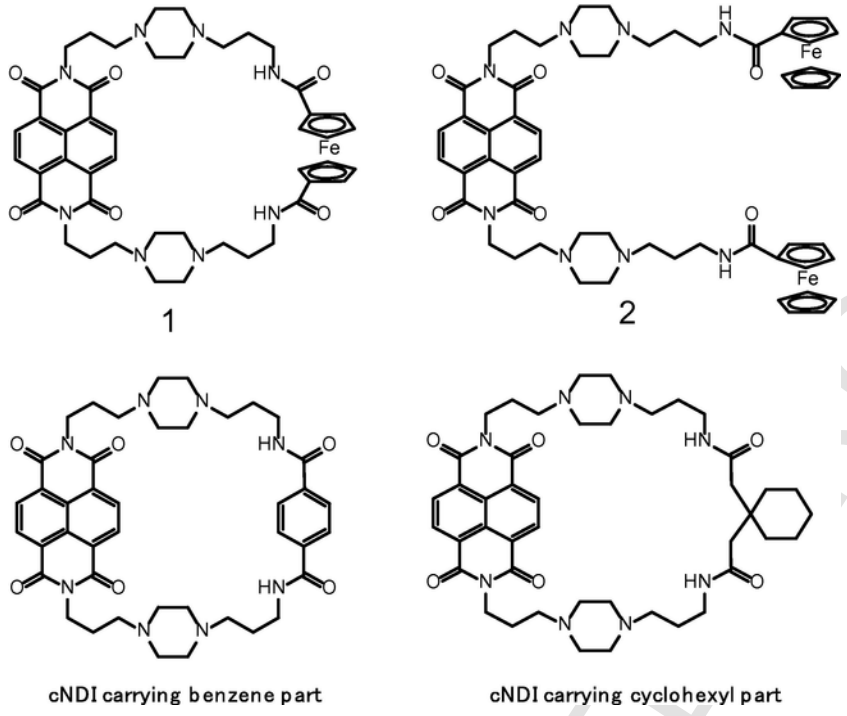

Fig. 1. Chemical structures of **1** and **2** with cNDI carrying benzene[9] or cyclohexyl[10] parts.

cause of the π-π overlapping between the benzene ring and nucleic base in the loop part of the G-quadruplex DNA. However, the benzene ring of cyclic ligands can go through the dsDNA base pair, resulting in intercalation such as bis-intercalation or catenation and, thus, the selectivity of cyclic ligands to G-quadruplex DNAs over dsDNA is reduced.

To address the above challenges and discover suitable cyclic ligands that selectively bind to G-quadruplex DNAs over dsDNA, we designed and synthesized a new cyclic ligand by cyclization using thick and rigid substituent such as ferrocene. We predicted that the ferrocene in the cyclic ligand might facilitate its binding with G-quadruplex loop through π-π overlapping and at the same time, the ferrocene moiety would prevent the intercalation or catenation binding with dsDNA. On the other hand, the thickness and rigidity of the ferrocene moiety should strengthen the cyclic structure and decrease the flexibility, and thereby reduce the binding to dsDNA. With this aim in mind, we synthesized cyclic ferrocenylnaphthalene diimide (cFND, **1**) by connecting NDI and ferrocene through an alkyl chain, piperazine, and amide group. The amide part of the linker chain of **1** may reduce the binding affinity to dsDNA because one face of the intercalator (NDI moiety) covered the hindered alkyl chain and, consequently, reduced intercalation to dsDNA. Furthermore, these new types of cyclic molecules may facilitate end stacking onto the G-quartet plane using a single face of the NDI moiety or both faces of NDI or ferrocene moiety. In this study, we also investigated compound **2**, which was reported to be a dsDNA binder that exhibits threading intercalation[15] with different types of G-quadruplex DNAs and dsDNAs, as a negative control to strengthen the evidence supporting the macrocyclization approach. We attempted to differentiate the binding properties of cyclic **1** and non-cyclic **2** with the DNAs and determine their selectivity towards the G-quadruplex DNA.

We aimed to determine the selectivity of **1** and **2** towards G-quadruplex DNAs and dsDNA, by examining the interaction of these ligands with G-quadruplex DNA carrying a human telomeric region (a-core and a-coreTT), promoter region (*c-myc* and *c-kit*), or thrombin-binding aptamer (TBA) and dsDNA. These different conformations of G-quadruplex DNAs were confirmed using circular dichroism spectra. A detailed evaluation of the selective binding of compound **1** and **2** with the G-quadruplex DNAs over dsDNA was carried out using ultraviolet–visible (UV–vis) titration, circular dichroism (CD) titration, CD melting, and UV–vis melting, as well as fluorescence resonance energy transfer (FRET) melting, topoisomerase I isomerase, and telomeric repeat amplification protocol (TRAP) assays.

To investigate the binding properties of **1** and **2** with various G-quadruplex DNAs and dsDNA, spectrophotometric titrations were carried out. In particular, we focused our attention on differentiating the binding properties between G-quadruplex DNAs and dsDNA, as well as the telomeric and non-telomeric G-quadruplex DNA. Fig. 2A depicts an example of the interaction between **1** and the human telomere G-quadruplex DNA (a-core) in K^+ ion, which revealed that the highest absorption was at 384 nm. After adding the pre-annealed a-core DNA to **1**, large hyperchromicities (45–60%) and small red-shifts (3–8 nm) were observed, which indicate the strong stacking interaction and specific mode of binding with G-quadruplex DNAs.[10] On the other hand, the interaction of **1** with dsDNA showed hypochromic (25–30%) and red (2–4 nm) shifts that were smaller than those observed with the G-quadruplex DNAs. This result suggests that this compound is not a good dsDNA binder (Fig. 2B). The Scatchard plot (Fig. 2C) of the G-quadruplex DNA was analyzed using the McGhee–von Hippel Scatchard equation to obtain a binding constant (K) and the ratio of **1** per DNA n value.[16] Furthermore, the nK values of the dsDNA were estimated using the Benesi–Hildebrand method because the binding saturation of **1** with dsDNA was not observed.[17] Compound **1** showed a binding affinity with G-quadruplex DNAs in the range of 10^6 M^{-1} with a stoichiometry of 2:1 (ligand/DNA). Furthermore, **1** did not show any significant binding affinity to dsDNA in the range of 10^4 M^{-1} order, which indicates that its

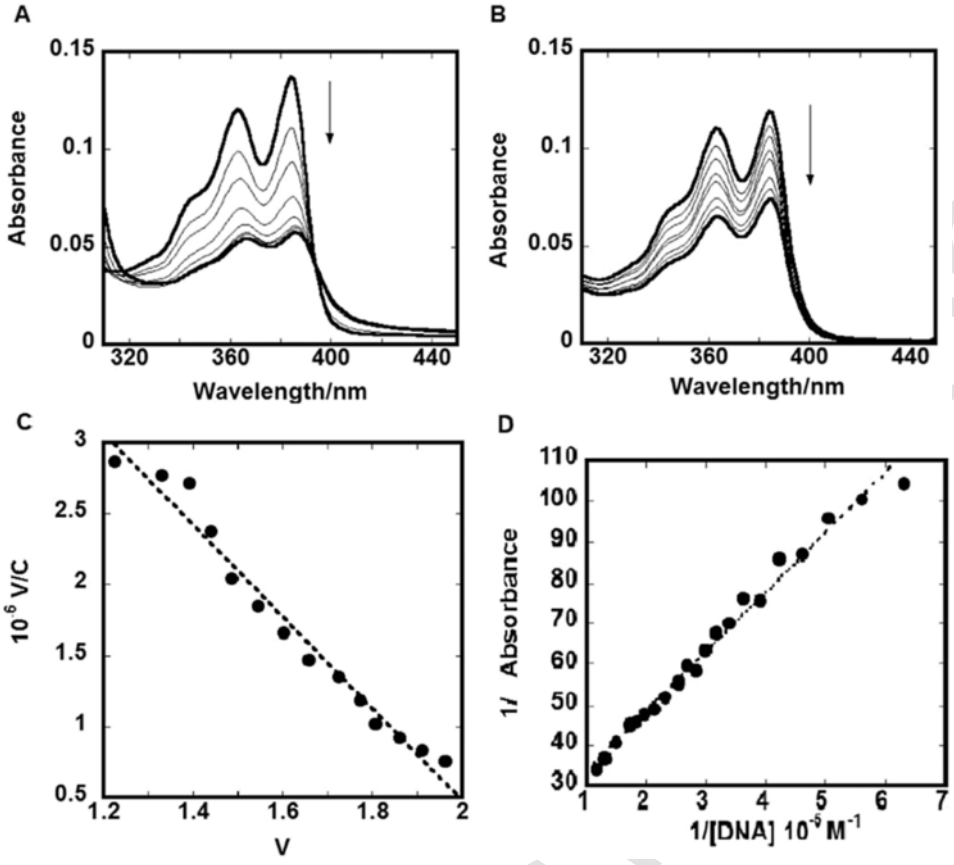

Fig. 2. Spectral shifts of 5 μM **1** on titration with 0, 1.4, 2.9, 4.4, 5.8, 8.7 and 14 μM a-core (A) or 0, 2, 5, 10, 20, 30, and 40 μM dsDNA (B) in 100 mM AcOH-AcOK buffer (pH 5.5) containing 100 mM KCl. Scatchard plots for binding of **1** to a-core (C) and Benesi-Hildebrand plot for binding of **1** to dsDNA (D).

specificity to G-quadruplex was approximately 50-fold higher than that to dsDNA.

As shown in Table 1, the binding constants in the K^+ ion were $K = 3.4 \times 10^6$ M^{-1} for a-core (mixed hybrid type),[18] $K = 2.6 \times 10^6$ M^{-1} for a-coreTT (hybrid type-2),[19] $K = 2.0 \times 10^6$ M^{-1} for TBA (antiparallel chair type),[20] $K = 2.0 \times 10^6$ M^{-1} for *c-kit* (parallel propeller type),[21] and $K = 1.9 \times 10^6$ M^{-1} for *c-myc* (parallel type)[22] with **1**, which were 50, 35, 26, 26, and 25 times higher binding preferences over ds-DNA ($K = 7.5 \times 10^4$ M^{-1}) respectively.

Table 1
Binding parameters and melting temperatures of **1** and **2** with a-core, a-coreTT, c-kit, c-myc, TBA, and dsDNA.

DNAs	10^{-6} K/M^{-1} (*n*)[a]		Tm/°C	ΔTm/°C	
	1	**2**		**1**	**2**
a-core	3.4 ± 0.3 (2.1)[b]	1.4 ± 0.3 (2.9)[b]	69[d]	10	5
a-coreTT	2.6 ± 0.3 (2.1)[b]	1.6 ± 0.2 (2.5)[b]	64[d]	7	6
TBA	2.0 ± 0.3 (1.4)[b]	1.9 ± 0.1 (2.8)[b]	51[d]	5	8
c-kit	2.0 ± 0.2 (2.3)[b]	2.0 ± 0.1 (4.0)[b]	54[e]	18	15
c-myc	1.9 ± 0.4 (2.4)[b]	1.8 ± 0.3 (3.4)[b]	70[f]	17	18
dsDNA	0.075[c]	1.0 ± 0.1 (3.0)[b]	49[d]	2	3

~~[g][ligand]:[DNA] = 2:1 in 100 mM AcOH-AcOK buffer (pH 5.5) in 5.0 mM KCl.~~

~~[a] 100 mM AcOH-AcOK buffer (pH 5.5) and 100 mM KCl.~~

~~[b] Scatchard analysis (*K* and *n*).~~

~~[c] Bensi-Hildebrand analysis (*nK*).~~

~~[e] [ligand]:[DNA] = 2:1 in 100~~

~~[f] [ligand]:[DNA] = 2:1 in 100~~

[a] 100 mM AcOH-AcOK buffer (pH 5.5) and 100 mM KCl.
[b] Scatchard analysis (K and n).
[c] Bensi-Hildebrand analysis (nK).
[d] [ligand]:[DNA] = 2:1 in 100 mM AcOH-AcOK buffer (pH 5.5) in 100 mM KCl.
[e] [ligand]:[DNA] = 2:1 in 100 mM AcOH-AcOK buffer (pH 5.5) in 20 mM KCl.
[f] [ligand]:[DNA] = 2:1 in 100 mM AcOH-AcOK buffer (pH 5.5) in 5.0 mM KCl.

The binding stoichiometry of **1** with the G-quadruplex DNA was estimated at 2:1 using a Scatchard plot (Supporting information Fig. S4), which may correspond to end-stacking binding to the external G-quartet planes. In Table 1, the binding constant data indicate that **1** had a binding affinity that was almost similar to that its affinity with different types of G-quadruplex DNAs. We found similar results in the FRET melting assay, which showed that the binding activities of **1** with the different G-quadruplex structures were comparable (Supporting information Fig. S5).[23] The binding constant and stoichiometry of **1** with G-quadruplex DNAs were consistent with the previous results obtained by Czerwinska et al.[10] It seems that the binding of **1** with the G-quadruplex DNAs may completely overlap with the G-tetrads. Moreover, the amide part of the linker chain of **1** may be more compatibility and, therefore, bind specifically with the G-quartet plane. However, we clearly observed that the binding of **1** with ds-DNA reduced more than its binding with G-quadruplex DNA did due to the linker chain of the ~~cFNDI~~ derivatives and the NDI or ferrocene moieties, which also prevented its binding to dsDNA.

In contrast, compound **2** exhibited a lower binding affinity to the G-quadruplex DNAs ($K = 1.4 \times 10^6$ M^{-1}) than **1** did. In addition, compound **2** showed a trend of stoichiometry that was similar to that of **1** because the binding of **2** with the G-quadruplex DNAs might not have completely overlapped with the G-tetrads, as opposed to the complete overlap observed with **1**. However, **2** still showed a higher affinity to dsDNA ($K = 1.0 \times 10^6$ M^{-1}) than **1** did because of

DNA and dsDNA clearly explains the specificity and selectivity of these ligands.

CD spectroscopy emerged as a useful technique for investigating the binding interaction of **1** and **2** with the G-quadruplex DNA (annealed with K^+ buffer) structure chromophore. We focused on the hybrid, parallel, and antiparallel G-quadruplex DNAs to investigate the interaction between the ligands and various G-quadruplex topologies. The CD spectra of the human telomere G-quadruplex DNAs (a-core and a-coreTT) revealed positive, negative, and shoulder peaks at 290, 240, and 265 nm, respectively (Fig. 3A and B) in buffer containing 100 mM KCl. This result indicates a mixed hybrid type (hybrid-1 and -2) for the a-core and hybrid-2 types for a-core TT in the G-quadruplex DNA structures.[25,26] Following the addition of **1** or **2**, a dose-dependent increase in the CD signals was observed, suggesting that the pre-folded mixed hybrid type (hybrid-1 and hybrid-2) and hybrid-2 type G-quadruplex DNA structures were retained. However, the TBA G-quadruplex DNA (Fig. 3C) revealed a negative band at 250 nm and a positive peak at 290 nm, suggesting an anti-parallel chair type G-quadruplex structure.[27] Following the addition of **1**, the positive peak at 290 nm gradually increased and the peak around 250 nm gradually decreased for TBA, indicating that the binding of **1** apparently caused no further significant change in the G-quadruplex DNA structure.[27] Remarkably, **1** caused a more significant increase in the ellipticity than **2** did, which was probably due to aggregation (Supporting information Fig. S6).

Furthermore, the promoter regions of the G-quadruplex DNA (*c-myc* and *c-kit*) exhibited a parallel structure in the presence of K^+ ions, which showed a negative peak at 241 nm, a positive peak centered around 262 nm, and a small shoulder peak at 290 nm (Fig. 3D and E).[28,29] The CD spectra gradually decreased at 241 and 262 nm with no other significant change in the spectrum following the addition of **1** or **2**, which suggests the ligand-dependent disruption stacking of the G-quadruplex DNA, which is the parallel structure, was retained. Interestingly, the *c-kit* structure showed a shoulder peak at 290 nm that increased slightly following the addition of the ligands, which was consistent with the results of a previous report.[30] Particularly, **1** revealed a more noteworthy decrease in ellipticity than **2** did (Supporting information Fig. S6). The binding stoichiometry of the Scatchard plot was confirmed to be 2:1 using a Job plot analysis for **1** and **2** with G-quadruplex DNA (Supporting information Figs. S7 and S8).[31]

To find out more details about the binding modes of these ligands, we carried out a topoisomerase I assay. Topoisomerase-based gel assays are widely recognized method used to evaluate ligands for their ability to intercalate into DNA.[32] We used a topoisomerase I assay to confirm the intercalation of **1** and **2** with supercoiled DNA. The topoisomerase I enzyme unwinds the supercoiled DNA into relaxed DNA. However, in the presence of the intercalator, the relaxed DNA re-converted into supercoiled DNA while the groove binder cannot re-supercoil DNA because of the negligible DNA unwinding with the binding.[33] In Fig. S9, the gel electrophoresis indicates that the relaxed plasmid DNA, pU19 completely re-supercoiled with compounds **1** and **2** in the presence of topoisomerase I enzyme, indicating that both compounds are DNA intercalators. In contrast, the groove binder did not show intercalating behavior. Cyclic structured compounds unwind the DNA and lengthen its structure because cyclic structured compounds require the DNA strands to dissociate. We previously reported that cyclic compounds show a slow dissociation rate from the duplex structure.[12] We also reported that cyclic-NDI derivatives can re-supercoil plasmid DNA,[9,10] which is consistent with the results of our present study.

Thermal stabilization of the DNA structure following binding with **1** or **2** was examined (2:1, ligand/DNA ratio) using CD and UV–vis melting assays using the specific detection wavelengths of the DNAs in the absence and presence of the molecules. All the thermal denaturation was monitored at the wavelengths of maximum CD intensity. Without compound **1**, the T_m value was recorded at approximately 69 and 63 °C for a-core and a-coreTT, respectively (Table 1, Fig. 4A and B) with an ellipticity at 290 nm. After the addition of **1**, the telomeric DNA quadruplex increased the thermal stability by 10 and 7 °C for the a-core and a-coreTT, respectively. At 290 nm wavelength, **1** increased the T_m of TBA by 5 °C (Table 1 and Fig. 4C), which are consistent with the results of previous reports.[23,27]

At a high salt concentration, the *c-kit* and *c-myc* G-quadruplex DNAs were highly stable, and the baseline curve was not achieved even at temperatures above 90 °C, but it was not possible to measure an accurate T_m in this case. Therefore, we measured the stability of *c-kit* and *c-myc* G-quadruplex DNAs at a low salt concentration. Compound **1** increased the T_m of *c-kit* by 18 °C and that of *c-myc* by 17 °C (Table 1 and Fig. 4D and E), which were monitored at 263 nm under K^+, supporting the results of our previous reports.[29,30] On the other hand, the UV–vis melting study of **1** with dsDNA revealed that the T_m increase by 2 °C, indicating that **1** was more highly stabilized with the G-quadruplex DNA than it was with dsDNA (Table 1, Supporting information Fig. S10). Compound **2** showed a lower melting profile with the G-quadruplex DNA than **1** did, and **2** also exhibited a higher T_m of up to 3 °C with dsDNA (Table 1, Supporting information Figs. S11 and S12), indicating its intercalation into the dsDNA. Remarkably, the CD melting studies indicated that compound **1** showed a stabilization with the promoter G-quadruplex that was almost two times higher than that observed with the telomeric (a-core and a-coreTT) or TBA G-quadruplex DNAs, and showed an approximately nine times higher order of specific stabilization than it did with the dsDNA. Considering our present results, we strongly conclude that the incorporation of ferrocene into the cyclic NDI derivatives likely improved their stability with the G-quadruplex DNAs. Furthermore, compounds **1** and **2** showed higher ΔTm values than those obtained with previously investigated ligands (approximately 2 or 9 °C for cyclic NDI with cyclohexyl and benzene parts, respectively, Table 1).

Based on the results of the binding and thermal stabilization studies, TRAP assays were performed to further investigate compounds **1** and **2**. The investigation showed that **1** is a strong inhibitor of telomerase at a sub-micromolar range with an IC_{50} of 0.4 μM (Supporting information, Fig. S13) whereas **2** showed an IC_{50} of 25 μM (unpublished data). The telomerase inhibitory activity of **1** was approximately 63-times higher than that of **2** was, and this result is in agreement with that of the binding affinity and thermal stability. Since the inhibitory effect was much higher than expected, the ferrocene moiety of **1** might have contributed to inhibiting the telomerase access in some way.

In summary, the novel compound **1** was synthesized successfully using cyclization of NDI with ferrocene using another two-linker chain and its binding interaction with different types of G-quadruplex DNAs and dsDNA was investigated. Collectively, these results suggest that the cyclic molecule **1** with an appropriate linker chain might facilitate the development of specific binding interactions with G-quadruplex DNAs over that with dsDNA. Therefore, compound **1** could be considered as a better prototype of a promising and important class of ligands for G-quadruplex stabilization than the linear chain compound **2** is. In addition, this study demonstrates the usefulness of engineering compounds for potential therapeutic applications.

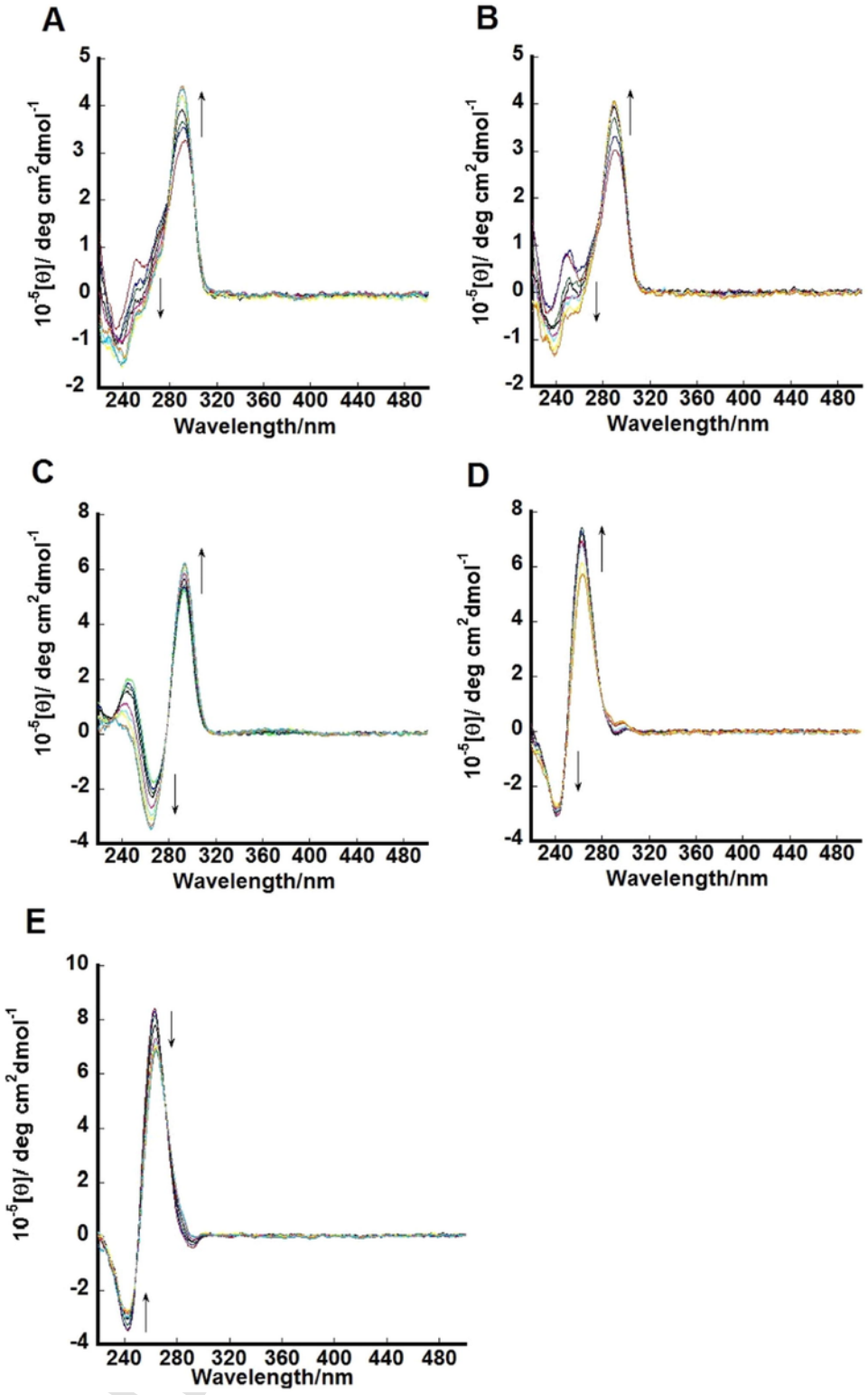

Fig. 3. CD spectra of 1.5 μM of a-core (A), a-coreTT (B), TBA (C), *c-kit* (D), or *c-myc* (E) in 100 mM AcOH-AcOK buffer (pH 5.5) containing 100 mM KCl in addition of **1** (0, 0.38, 0.75, 0.80, 2.25, and 3.00 μM with arrow direction) at 25 °C.

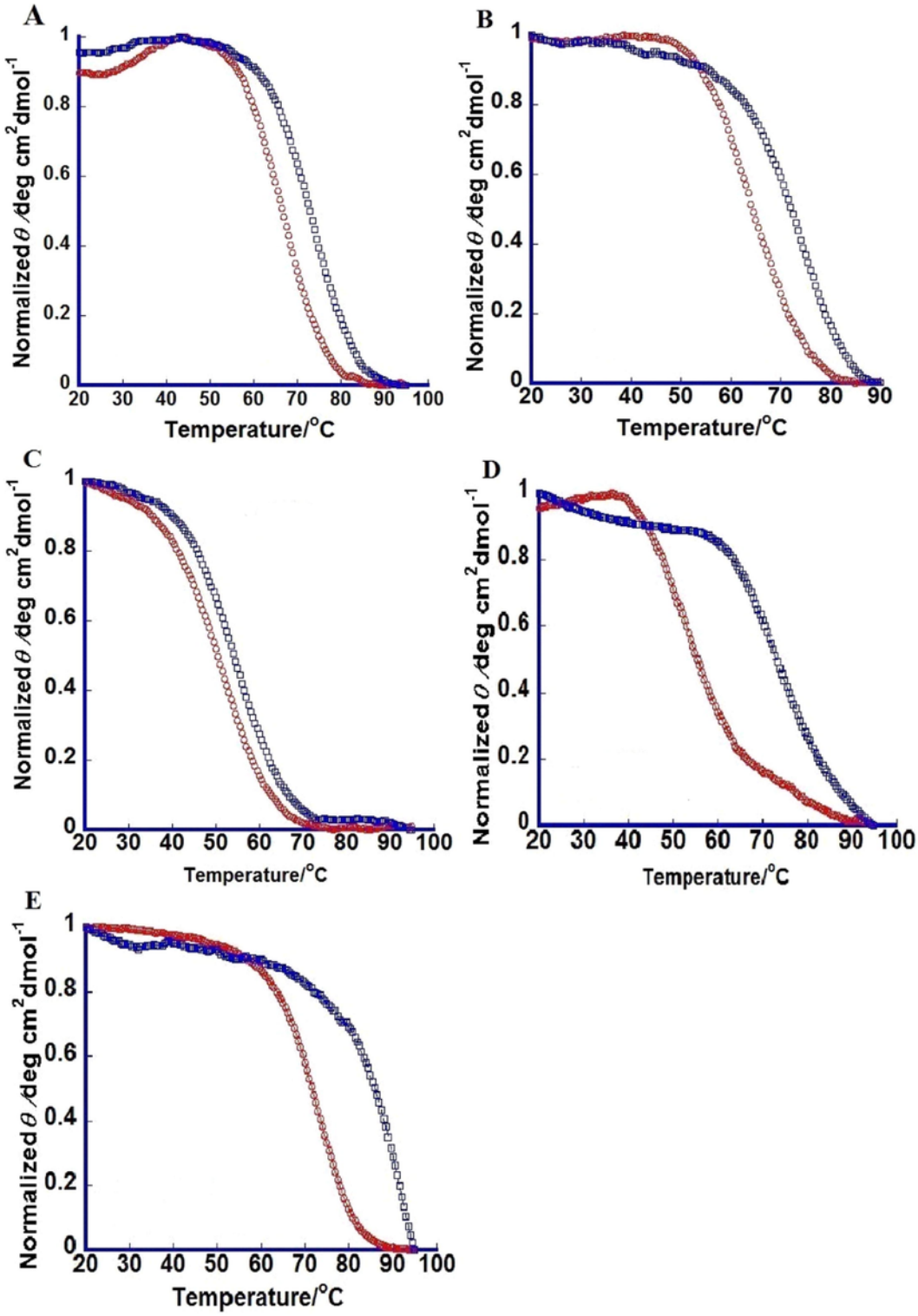

Fig. 4. Melting profiles for a-core (A), a-coreTT (B), TBA (C), *c-kit* (D), *c-myc* (E) in the absence (red curve) or presence (blue curve) of **1** with [**1**]: [DNA] = 2:1 in 100 mM AcOK-AcOH buffer (pH 5.5) containing 100 mM KCl (A–C), 20 mM KCl (D), or 5 mM KCl (E). (For interpretation of the references to colour in this figure legend, the reader is referred to the web version of this article.)

Acknowledgements

This work was supported by Grants-in-Aid for Scientific Research-KAKENHI, Challenging Exploratory Research (Grant No: 15K13748) of JSPS (Japan Society for the Promotion of Science).

A. Supplementary data

Supplementary data associated with this article can be found, in the online version, at http://dx.doi.org/10.1016/j.bmcl.2016.11.037.

References

1. S. Neidle, Therapeutic Applications of Quadruplex Nucleic Acid, 1st ed.Academic press, New York, 20121–15.
2. M.L. Bochman, K. Paeschke, V.A. Zakian, DNA secondary structures: stability and function of G-quadruplex structures, Nat Rev Genet 13 (2012) 770–780.
3. D.J. Patel, A.T. Phan, V. Kuryavyi, Human telomere, oncogenic promoter and 5'-UTR G-quadruplexes: diverse higher order DNA and RNA targets for cancer therapeutics, Nucleic Acids Res 35 (2007) 7429–7455.
4. J. Dai, M. Carver, D. Yang, Polymorphism of human telomeric quadruplex structures, Biochimie 90 (2008) 1172–1183.
5. P. Murat, Y. Singh, E. Defrancq, Methods for investigating G-quadruplex DNA/ligand interactions, Chem Soc Rev 40 (2011) 5293–5307.
6. T. Ou, Y. Lu, J. Tan, Z. Huang, K. Wong, L. Gu, G-Quadruplexes: targets in anticancer drug design, ChemMedChem 3 (2008) 690–713.
7. D. Monchaud, M.P. Teulade-Fichou, A hitchhiker's guide to G-quadruplex ligands, Org Biomol Chem 6 (2008) 627–636.
8. J.T. Davis, G-Quartets 40 years later: from 5′-GMP to molecular biology and supramolecular chemistry, Angew Chem Int Ed Engl 43 (2004) 668–698.
9. M.C. Nielsen, T. Ulven, Macrocyclic G-quadruplex ligands, Curr Med Chem 17 (2010) 3438–3448.
10. I. Czerwinska, S. Sato, B. Juskowiak, S. Takenaka, Interactions of cyclic and non-cyclic naphthalene diimide derivatives with different nucleic acids, Bioorg Med Chem 22 (2014) 2593–2601.
11. Y. Esaki, M.M. Islam, S. Fujii, S. Sato, S. Takenaka, Design of tetraplex specific ligands: cyclic naphthalene diimide, Chem Commun 50 (2014) 5967–5969.
12. M.M. Islam, S. Fujii, S. Sato, T. Okauchi, S. Takenaka, Thermodynamics and kinetic studies in the binding interaction of cyclic naphthalene diimide derivatives with double stranded DNAs, Bioorg Med Chem 23 (2015) 4769–4776.
13. M.M. Islam, S. Fujii, S. Sato, T. Okauchi, S. Takenaka, A selective G-quadruplex DNA stabilizing ligand based on cyclic naphthalene diimide derivative, Molecules 20 (2015) 10963–10979.
14. C. Marchetti, A. Minarini, V. Tumiatti, et al., Macrocyclic naphthalene diimides as G-quadruplex binders, Bioorg Med Chem 23 (2015) 3819–3830.
15. S. Takenaka, K. Yamashita, M. Takagi, Y. Uto, H. Kondo, DNA sensing on a DNA probe-modified electrode using ferrocenylnaphthalene diimide as the electrochemically active ligand, Anal Chem 72 (2000) 1334–1341.
16. J.D. McGhee, P.H. vonHippel, Theoretical aspects of DNA-protein interactions: co-operative and non-co-operative binding of large ligands to a one-dimensional homogeneous lattice, J Mol Biol 86 (1974) 469–489.
17. H.A. Benesi, J.H. Hildebrand, A spectrophotometric investigation of the interaction of iodine with aromatic hydrocarbons, J Am Chem Soc 71 (1949) 2703–2707.
18. A. Ambus, D. Chen, J. Dai, T. Bialis, R.A. Jones, D. Yang, Human telomeric sequence forms a hybrid-type intramolecular G-quadruplex structure with mixed parallel/antiparallel strands in potassium solution, Nucleic Acids Res 34 (2006) 2723–2735.
19. R. Hansel, F. Lohr, S.F. Trantırkova, E. Bamberg, L. Trantirek, V. Dotsch, The parallel G-quadruplex structure of vertebrate telomeric repeat sequences is not the preferred folding topology under physiological conditions, Nucleic Acids Res 39 (2011) 5768–5775.
20. J.X. Dai, M. Carver, L.H. Hurley, D.Z. Yang, Solution structure of a 2:1 quindoline-c-MYC G-quadruplex: insights into G-quadruplex-interactive small molecule drug design, J Am Chem Soc 133 (2011) 17673–17680.
21. M. Toro, R. Gargallo, R. Eritja, J. Jaumot, Study of the interaction between the G-quadruplex-forming thrombin-binding aptamer and the porphyrin 5,10,15,20-tetrakis-(N-methyl-4-pyridyl)-21, 23H-porphyrin tetratosylate, Anal Biochem 379 (2008) 8–15.
22. R.F. Macaya, P. Schultze, F.W. Smith, J.A. Roet, J. Feigon, Thrombin-binding DNA aptamer forms a unimolecular quadruplex structure in solution, Proc Natl Acad Sci USA 90 (1993) 3745–3749.
23. P. Ragazzon, J.B. Chaires, Use of competition dialysis in the discovery of G-quadruplex selective ligands, Methods 43 (2007) 313–323.
24. S. Sato, H. Kondo, T. Nojima, S. Takenaka, Electrochemical telomerase assay with ferrocenylnaphthalene diimide as a tetraplex DNA-specific binder, Anal Chem 77 (2005) 7304–7309.
25. A.T. Phan, V. Kuryavyi, K.N. Luu, D.J. Patel, Structure of two intramolecular G-quadruplexes formed by natural human telomere sequences in K+ solution, Nucleic Acids Res 35 (2007) 6517–6525.
26. K.N. Luu, A.T. Phan, V. Kuryavyi, L. Lacroix, D.J. Patel, Structure of the human telomere in K+ solution: an intramolecular (3+1) G-quadruplex scaffold, J Am Chem Soc 128 (2006) 9963–9970.
27. S. Nagatoishi, Y. Tanaka, K. Tsumoto, Circular dichroism spectra demonstrate formation of the thrombin-binding DNA aptamer G-quadruplex under stabilizing-cation-deficient conditions, Biochem Biophys Res Commun 352 (2007) 812–817.
28. J. Dash, P.S. Shirude, S.D. Hsu, S. Balasubramanian, Diarylethynyl amides that recognize the parallel conformation of genomic promoter DNA G-quadruplexes, J Am Chem Soc 130 (2008) 15950–15956.
29. C. Wei, Y. Wang, M. Zhang, Synthesis and binding studies of novel di-substituted phenanthroline compounds with genomic promoter and human telomeric DNA G-quadruplexes, Org Biomol Chem 11 (2013) 2355–2364.
30. V. Dhamodharan, S. Harikrishna, C. Jagadeeswaran, K. Halder, P.I. Pradeepkumar, Selective G-quadruplex DNA stabilizing agents based on bisquinolinium and bispyridinium derivatives of 1,8-naphthyridine, J Org Chem 77 (2012) 229–242.
31. R. Kieltyka, P. Englebienne, N. Miotessier, H. Sleiman, Quantifying interactions between G-quadruplex DNA and transition-metal complexes, in: P. Baumann (Ed.), G-Quadruplex DNA Methods and Protocols, 1st ed., Humana Press, c/o Springer Science+Business Media, LLC, 233 Spring Street New York, 2010, pp. 221–256.
32. P. Peixoto, C. Bailly, M.H. David-Cordonnier, Topoisomerase I-mediated DNA relaxation as a tool to study intercalation of small molecule into supercoiled DNA, Methods Mol Biol 613 (2010) 235–256.
33. R. Palchaudhuri, P.J. Hergenrother, DNA as a target for anticancer compounds: methods to determine the mode of binding and the mechanism of action, Curr Opin Biotechnol 18 (2007) 497–503.